

New *P*-wave first motion solutions for the focal mechanisms of the Rissani (Morocco) earthquakes of October 23^d and 30th, 1992

Ihsane BENSALD¹, Fida MEDINA^{1*}, Taj-Eddine CHERKAOUI^{1**},
Elisa BUFORN² & Youssef HAHOU³

1. Université Mohammed V – Agdal, Institut Scientifique, Département des Sciences de la Terre, Av. Ibn Batouta, B.P. 703 Agdal, Rabat, Morocco. *auteur correspondant : medina@israbat.ac.ma; ** chercheur associé.

2. Universidad Complutense, Facultad de Ciencias Físicas, Departamento de Geofísica y Meteorología, Madrid, Spain.

3. Centre National de la Recherche Scientifique et Technique, Quartier Ryad, B.P. 8027 Nations Unies, Rabat.

Nouvelles solutions des mécanismes au foyer des séismes de Rissani (Maroc) des 23 et 30 octobre 1992, basées sur le premier sens du mouvement des ondes P.

Résumé. Deux nouvelles solutions sont présentées pour les mécanismes au foyer des séismes de Rissani des 23 et 30 octobre 1992 (Tab. I ; Fig. 1), de magnitude $M_b = 5.2$, sur la base de la détermination du premier sens des ondes P de stations situées au Maroc (permanentes ou temporaires), en Espagne, en Algérie, en Tunisie et en Côte d'Ivoire (Fig. 2 ; Annexe). Les deux solutions correspondent à des décrochements avec des plans orientés E-W dextre et N-S senestre (Tab. II ; Fig. 3). Ces solutions, déterminées à l'aide du programme de Brillinger, sont proches de celles déterminées par Harvard à l'aide du *Centroid Moment Tensor*, mais les pendages des plans N-S dans les deux solutions, et le plan E-W dans un cas sont opposés (Tab. II ; Fig. 3). Les plans E-W auraient été les plans de faille principaux en raison de la présence de nombreuses failles normales paléozoïques ayant cette direction.

Introduction

On October, 23d and 30th, 1992, south-eastern Morocco, particularly the Tafilalt region (Fig. 1), was shaken by two strong earthquakes of magnitude $M_b = 5.2$, which caused 2 deaths and great damage along the Ziz valley between Erfoud and Rissani. Maximum intensities were VI-VII MSK (October, 23d) and VII MSK (October, 30th) in the epicentral area respectively (Cherkaoui 1993, Hahou *et al.* 2003). Both shocks have been located by the

International Seismological Centre (ISC) and Hahou *et al.* (2003) (Table I); the latest determination, performed by one of us (T.-E.C.), is based on additional data from the network of portable stations installed near Khénifra at that time, which was the closest to the epicentre. The epicentral coordinates are located at 31°21'40"N; 04°10'55"W (October, 23d) and 31°17'10"N; 04°20'49"W (October, 30th) (Fig. 1) and very shallow depth [2 km (\pm ERZ=5.4 km for both shocks)].

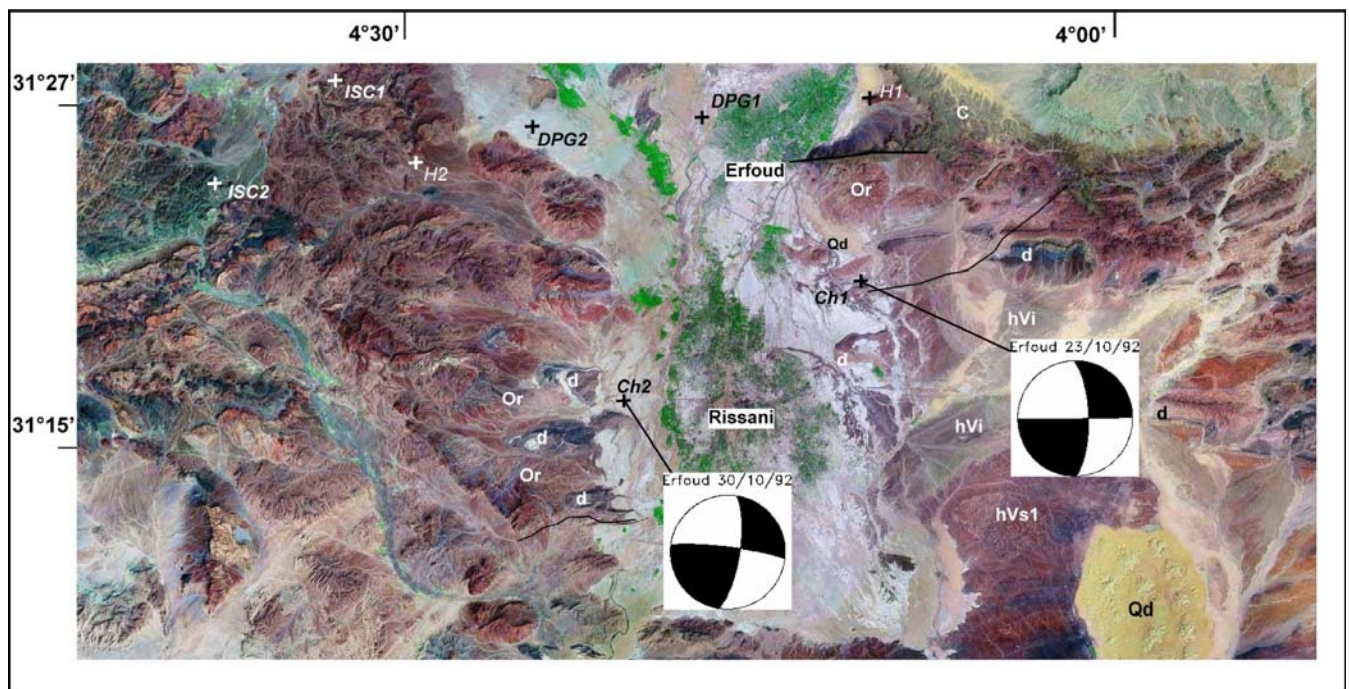


Figure 1. Satellite image of the Tafilalt region showing the main geological units and the epicentres of the events of October, 23d (1) and 30th (2), 1992. Geological units (after Destombes & Hollard 1986): Or, Ordovician; d, Devonian; hVi, Early Visean; hVs1, Late Visean; C, Cretaceous; Qd, Quaternary dunes. Determined epicentres: ISC, International Seismological Centre (Kew); DPG, Département de Physique du Globe (Rabat); Ch, Cherkaoui (1993); H, Hahou *et al.* (2003).

Table I. Epicentre location of the October, 23d and 30th earthquakes by different institutions and authors.

Date	Origin time	Coordinates	Depth (km)	Magnitude	Reference
23 October 1992	09:11:05	31°29' N; 04°33' W (31.483°N; 4.550°W)	5	Mb = 5.2	ISC
	09:11:12	31.466°N; 04.176°W	14	Md = 5.2	Hahou <i>et al.</i> (2003)
	09:11:08	31°21'40" N; 04°10'55" W (31.361°N; 4.181°W)	2	Mb = 5.2	This paper
30 October 1992	10:43:56	31°25' N; 04°38' W (31.416°N; 4.633°W)	8	Mb = 5.1	ISC
	10:44:02	31.432°N; 04.507°W	16	Md = 5.3	Hahou <i>et al.</i> (2003)
	10:43:58	31°17'10" N; 04°20'49" W (31.286°N; 4.346°W)	2	Mb = 5.1	This paper

Focal mechanisms of these events, determined by Harvard CMT solutions and Jabour (1993 in Hahou *et al.* 2003), correspond to strike-slip faulting along N-S, sinistral, and E-W, dextral, planes. Harvard CMT solutions are given in Table II and illustrated in Fig. 3. Hahou *et al.* (1993; their Fig. 3) show the solution of Jabour (1993) but do not indicate the parameters; with respect to the solution determined by Harvard, the attitude of the E-W plane appears to be the same, whereas the N-S is slightly steeper.

However, the Harvard's CMT solution is inconsistent with data of P wave at regional distances, due to the use of teleseismic data and a fixed depth (15 km) for shallow earthquakes. This led us to search a new solution based on P wave first motion data.

New Data

Our data have been directly read from several sources (Appendix):

- Seismograms of 9 portable stations that were installed at that time near Khenifra, during a survey related to the AI368/88 project.
- Paper seismograms available at the Institut Scientifique permanent stations (AVE, IFR, ANT, TIO and TAF) and portable station IMM.
- Digital data (short period) of Red Sísmica Nacional (Instituto Geográfico, Madrid, Spain), for Spanish stations at regional distances (less than 1000 km).
- Broad band data of Geofon network for European stations (epicentral distances 1000-2500 km).
- Paper copies provided by the Tunisian and Ivory Coast networks.
- Digital records provided by IPG/GEOSCOPE (station TAM).

As depicted in figure 2, the quality of readings of the first motions recorded by the main stations varies from excellent (Moroccan network) to poor (some Tunisian stations). The stations were chosen so as to cover all quadrants of the focal sphere, especially the southern and south-eastern quadrants, which are generally poorly covered.

Method

Fault plane solutions were obtained from first motion of P waves, using an the algorithm developed by Brillinger *et al.* (1980) to estimate fault plane orientation, their errors and score for both shocks. A crustal specific model for Morocco, formed by two flat layers (12 km and 18 km respectively) with constant P velocity 6.0 km/s and 6.75 km/s over a semi-infinite space (velocity 7.8 km/s), it has been used to estimate the take off angle for stations at regional distances (less than 1000 km). These velocities are constrained by seismic refraction data from Schwarz & Wigger (1988) and Wigger *et al.* (1992). For stations at larger distances, we have used a spherical Earth model (IASPEI model).

Results

The best solution for the October, 23d shock (Tab. II; Fig. 3A), is strike-slip faulting with a slight normal component. The planes are oriented 359°; 71°; -1° (sinistral) and 89°; 89°; -161° (dextral). The P axis is oriented 316°; 14° and the T axis is at 223°; 13°. Estimations of errors for P and T axis are less than 15°. The number of polarities is 30 with a score of 0.97.

With respect to Harvard CMT and Jabour's solution, ours shows an opposite direction of dip for the N-S plane and a steeper E-W plane, constrained by the position of stations TAM, LIC, TIO, CIA and ENIJ.

The solution for the October, 30th shock (Tab. II; Fig. 3B), is also strike-slip faulting but with a reverse component. The planes are oriented 9°; 73°; 7° (sinistral) and 277°; 83°; 163° (dextral). The P axis is oriented 324°; 7° and the T axis is at 232°; 16°. This solution is well constrained with errors less than 15°, the score is 1.0 but we have less observations in comparison with the shock of the 23d. The dip of the E-W plane is tightly constrained by stations OUK, TAZ and CHIE. Both planes are of opposite dip with respect to Harvard's solution.

Preliminary comparison with geological (Margat 1960, Destombes & Hollard 1986) and seismic-reflection data (Robert-Charrue & Burkhard 2006, Baïdder 2007, Toto *et al.* 2007), shows that the epicentres of the main shocks are

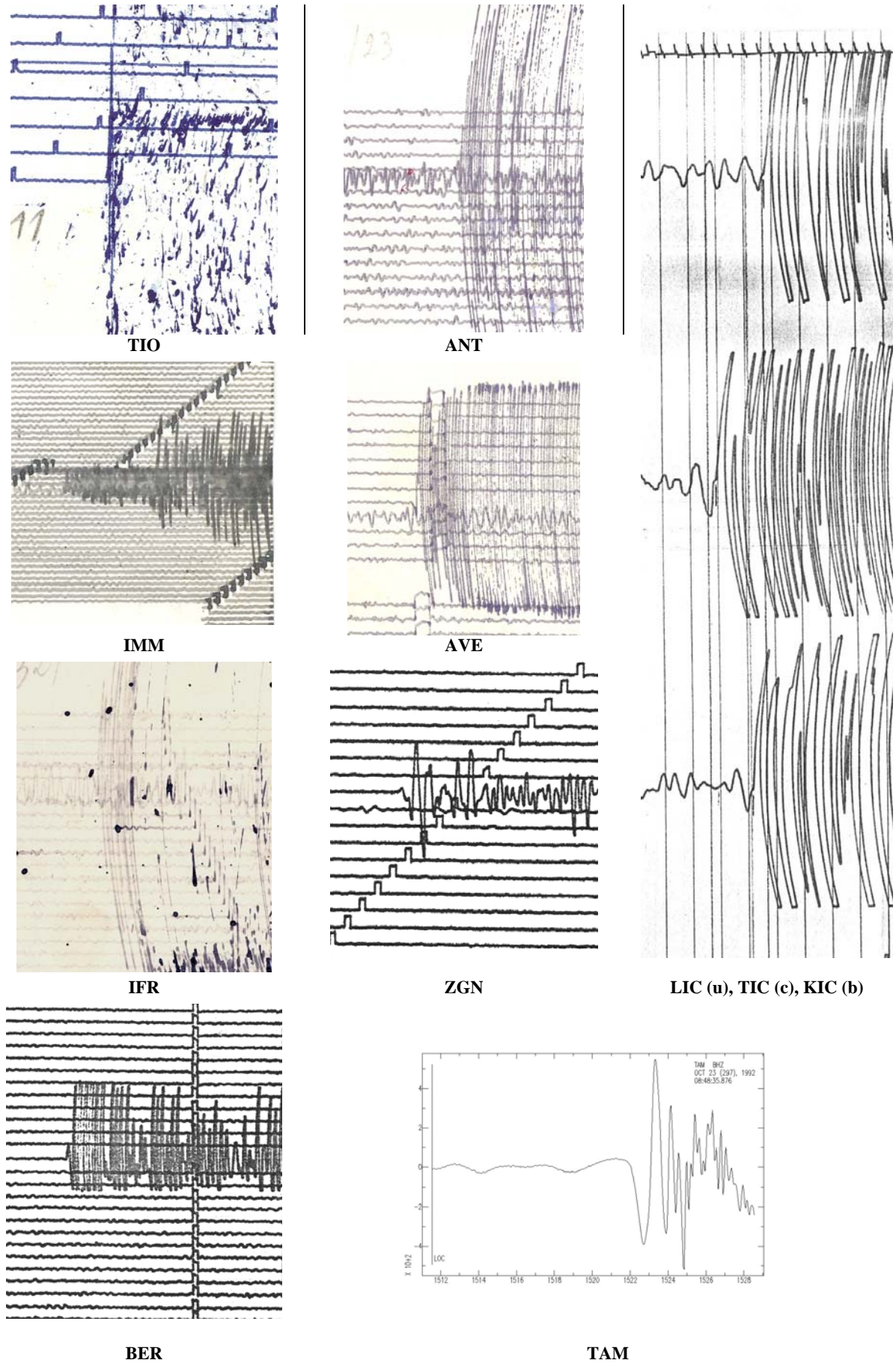


Figure 2. Close-up images of the first motion of the October, 23th event at various stations used for the determination of the focal mechanisms.

Table II. Parameters of the focal mechanism solutions determined by Harvard and the present authors. Φ =strike ; δ = dip ; λ =slip.

Event	Plane A ($^{\circ}$) (Φ, δ, λ)	Plane B ($^{\circ}$) (Φ, δ, λ)	P axis ($^{\circ}$) (Tr; pl)	T axis ($^{\circ}$) (Tr; pl)	Method	Reference
23 October 1992	187; 69; 012	92; 78; 158	141; 07	048; 24	CMT	Harvard
	359±9; 71±9; -1±11	89±11; 89±10; -161±9	316±10; 14±10;	223±09; 13±09	FM	This paper
30 October 1992	090; 72; 176	181; 87; 018	314; 10	047; 15	CMT	Harvard
	9±11; 73±14; 7±11	277±12; 83±10; 163±14	324±12 07±12	232±11 16±12;	FM	This paper

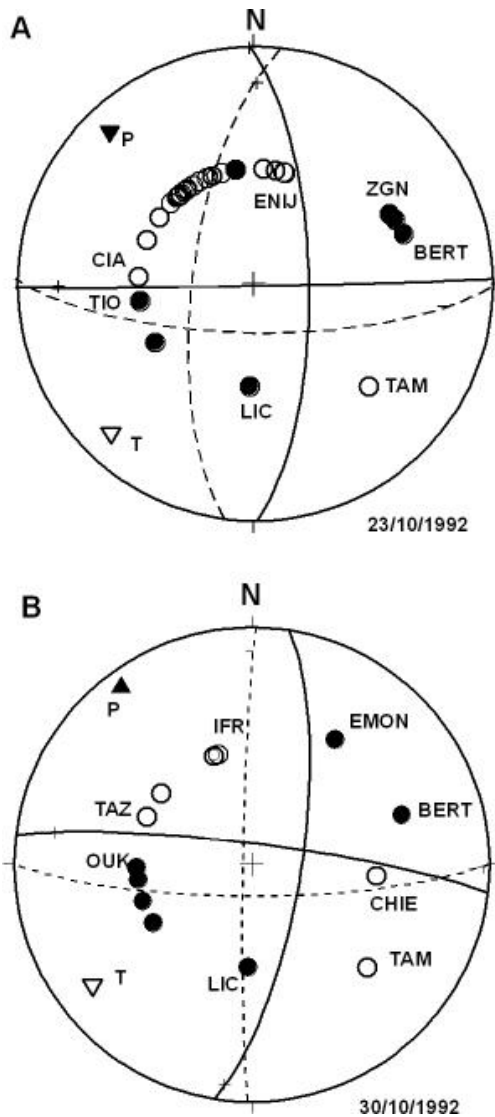


Figure 3. Focal mechanisms (Schmidt net, lower hemisphere) of the October, 23^d (upper diagram) and 30th (lower diagram), 1992. Empty circles = dilatations; full circles = compressions; empty triangle = T axis; full triangle = P axis.

located in a folded and faulted area, mainly related to the Variscan orogeny which is also affected by WNW-ESE to E-W striking, vertical to moderately dipping, normal faults such as the Erfoud Fault (Fig. 1, EF). As the E-W seismic profile studied by Toto *et al.* (2007) shows no N-S faults, it

appears that one of these WNW-ESE to E-W faults may have been reactivated during the Alpine orogeny of the High Atlas with a strike-slip motion, and is seismically active at present (Cherkaoui 1988). The precise relationship of the faults and main shocks and aftershocks is currently under study.

Acknowledgements

This study has been partially supported by the Universidad Complutense de Madrid, project AE1/09-16586. We acknowledge the help of several colleagues in Tunisia, Ivory Coast and France, who gently provided copies of seismograms. We are particularly indebted to Pr. Denis Hatzfeld (IRIGM, Observatory of Grenoble) for his review and for providing the seismograms of the microseismic campaign carried out in the Khenifra province in collaboration with the Scientific Institute (T.-E. Cherkaoui).

References

Baidder L. 2007. *Structuration de la bordure septentrionale du Craton Ouest-Africain du Cambrien à l'Actuel: cas de l'Anti-Atlas oriental du Maroc*. Thèse d'Etat, Univ. Hassan II-Aïn Chock, Fac. Sci., 211 p.

Brillinger D.R., Udias A. & Bolt B.A. 1980. A probability model for regional focal mechanism limitrophes, *Bull. Seism. Soc. Am.*, 70, 149-170.

Cherkaoui T.-E. 1988. Fichier des séismes du Maroc et des régions voisines 1901-1984. *Trav. Inst. Sci.*, sér. Géol. & Géogr. phys., 17, 158 p. + carte h.t.

Cherkaoui T.-E. 1993. Etude sismologique du séisme du 30 octobre 1992 à Rissani. Rapport inédit; Dpt. de Phys. Globe; Inst. Sci., Rabat, 18 p.

Destombes J. & Hollard H. 1986. Carte géologique du Maroc au 1 / 200 000, feuille Tafilalt-Taouz. *Notes & Mém. Serv. Géol. Maroc*, n° 244.

Hahou Y., Jabour N., Oukemini D. & El Wartiti M. 2003. The October 23; 30, 1992 Rissani earthquakes in Morocco: Seismological, macroseismic data. *Bull. Int. Inst. Seismol. Earthq. Eng.*, Special Edition, 85-94.

International Seismological Centre (1992). Bulletin, October 1992, Kew (U.K.), pp. 202-203 and 353-355.

Margat J. 1960. Carte hydrogéologique de la plaine de Tafilalt au 1/50.000. I- Géologie et piézométrie. *Publ. Serv. Géol. Maroc*, n°150.

Robert-Charrue C. & Burkhard M. 2008. Inversion tectonics interference pattern and extensional fault-related folding in the Eastern Anti-Atlas, Morocco. *Swiss J. Geosci.*, 101, 397-408.

Schwarz, G.; Mehl, H.G.; Ramdani, F. & Rath, V. (1992): Electrical resistivity structure of the eastern Moroccan Atlas system and its tectonic implications. *Geol. Rundsch.*, 81, 1, 221-235.

Toto E.A., Kaabouben F., Zouhri L., Belarbi M., Benammi M., Hafid M. & Boutib L. 2007. Geological evolution and structural style of the Palaeozoic Tafilalt sub-basin, eastern Anti-Atlas (Morocco, North Africa). *Geol. J.*, DOI: 10.1002/gj.1098.

Wigger, P.; Asch, G.; Giese, P.; Heinsohn, W.-D.; El Alami, S.O. & Ramdani, F. (1992): Crustal structure along a traverse across

the Middle and High Atlas mountains derived from seismic refraction studies. *Geol. Rundsch.*, 81, 1, 237-248.

Manuscript received 29 October 2009
Accepted in revised form 25 December 2009

Appendix. List of stations used for the determination of the solutions, their epicentral distance, the take-off angle and the first motion observed (D=down; U=up).

Station code	Octobre 23, 1992 event			Octobre, 30, 1992 event		
	Epicentral distance (km)	Take-off angle	Polarity	Epicentral distance (km)	Take-off angle	Polarity
DRA	162	39	D			
TOUR	164	39	D			
TAMK	181	39	D			
ITZ	183	39	D			
KEB	183	39	D			
TAO	205	39	D			
FIL	191	39	D			
CLZ				205	40	D
AJD	215	39	D			
SRO	211	39	D			
TAZ	236	39	D	225	40	D
MSH	248	39	D			
IFR	256	39	D	259	40	D
TIO	298	39	U	281	40	U
ZER	319	39	D			
AVE	373	39	D	365	40	D
CIA	435	39	D			
RSA	420	39	D			
ANTZ	635	39	U	617	40	U
KER	190	39	D			
OUK				336	40	U
RTC	386	39	D			
EGUA	612	39	D			
EHUE	733	39	D			
EMEL	453	39	D			
ENIJ	650	39	D			
EPRU	631	39	U			
CFTV				993	40	U
BERT	1275	56	U	1292	57	U
ZGN	1432	54	U			
TIC	2736	36	U	2727	36	U
TAM	1351	55	D	1356	55	D
TROT	1362	55	U			
EMON				1673	53	U
CHIE				2166	44	D